



OPEN

Sporadic colon cancer murine models demonstrate the value of autoantibody detection for preclinical cancer diagnosis

SUBJECT AREAS:
AUTOIMMUNITY
DIAGNOSTIC MARKERS
CANCER SCREENING
COLORECTAL CANCER

Rodrigo Barderas^{1*†}, Roi Villar-Vázquez^{1*}, María Jesús Fernández-Aceñero², Ingrid Babel¹, Alberto Peláez-García¹, Sofía Torres¹ & J. Ignacio Casal¹

Received
21 June 2013

Accepted
23 September 2013

Published
15 October 2013

Correspondence and requests for materials should be addressed to J.I.C. (jicasal@cib.csic.es)

* These authors contributed equally to this work.

† Current address: Biochemistry and Molecular Biology I Department. Facultad de Ciencias Químicas. Universidad Complutense de Madrid. 28040 Madrid.

¹Department of Cellular and Molecular Medicine. Centro de Investigaciones Biológicas (CSIC). 28040 Madrid. Spain, ²Pathology Department. Fundación Jiménez Díaz. Madrid. Spain.

Although autoantibody detection has been proposed for diagnosis of colorectal cancer, little is known about their initial production and development correlation with cancer progression. Azoxymethane/dextran sodium sulfate (AOM/DSS)-treated mice developed colon adenocarcinoma in the distal colon similar to human sporadic colon cancer. We assessed this model together with AOM and DSS-only models for their applicability to early detection of cancer. All AOM/DSS-treated mice produced autoantibodies to tumor-associated antigens analogous to those observed in human colon cancer patients. Autoantibody response was related to tumor antigen overexpression. Cancer autoantibodies were detected 21 days after starting treatment, when no malignant histopathological features were detectable, and they increased according to tumor progression. When carcinogenesis was induced separately by AOM or DSS, only those mice that developed malignant lesions produced significant levels of autoantibodies. These findings demonstrate that autoantibody development is an early event in tumorigenesis and validates its use for preclinical colon cancer diagnosis.

Cancer patients develop an immune humoral response against tumor-associated antigens (TAAs). Autoantibody responses have been mainly associated to cancers with an elevated inflammatory component such as colon^{1–3}, prostate⁴, ovarian^{5,6}, lung^{7,8} or breast cancer⁹, among others. In addition to elevated specificity and sensitivity, advantages of this strategy include easy and minimally invasive sample collection for diagnosis. Moreover, the long stability of the antibody molecules allows for retrospective studies in samples stored for long periods^{10,11}. We hypothesized that murine colon cancer models could mimic the human humoral response to cancer and provide us with a clear insight into the production, kinetics and evolution of autoantibody development, including a clear answer to their potential application to cancer diagnosis in preclinical and early colon cancer stages.

We used azoxymethane (AOM) and dextran sodium sulfate (DSS), individually or in combination, to generate different inducible mouse models of colon cancer in order to study the effect of carcinogenicity and/or inflammation on the induction of autoantibodies. AOM is a chemical agent that initiates cancer by alkylation of DNA, favoring the introduction of mutations¹². Intraperitoneal administration of 3 to 6 AOM-only injections induces the development of spontaneous tumors in distal colon within 7–10 months depending on the mouse strain¹³. On the other hand, DSS supply in drinking water induces inflammatory cell infiltration of the mucosa propria, ulceration and bloody diarrhea¹⁴. DSS disrupts the colon epithelial lining, provoking severe colitis and ulcerative colitis-like neoplasia lesions mainly found in the distal colon^{15,16}. Administration of 3 to 4 and up to 9 DSS cycles in drinking water results in the development of colorectal dysplasia and adenocarcinoma in a subset of treated mice^{14,17}. Number, severity of lesions and percentage of affected mice depends on the mouse strains^{14,17,18}.

The combined treatment with AOM/DSS is currently used as a common mouse model of colitis-associated colon cancer (CAC). Tumors induced by AOM/DSS occur preferentially at the distal part of the colon, which is the predominant localization of spontaneous colorectal cancer (CRC) in humans. Although metastasis is very rare in this model¹⁹, many steps in cancer development including formation of aberrant crypt foci, polyps, adenomas and carcinomas are shared between CRC and CAC. It has been extensively used for the study of inflammation and its association with colon cancer development^{20,21}. This model has been very useful for the elucidation of the role of TNF- α , IL6, NF κ B and other molecules in the initiation and promotion of inflammation-associated tumor growth (see²² for a review), but it has not been applied for autoimmunity and biomarker studies. Tumor



development takes less than 10 weeks and the number and severity of lesions depends on the susceptibility to AOM and DSS of the mouse strain¹². Ten weeks should be long enough for the production and evaluation of specific antibodies to tumor antigens.

In addition, in this report we tested a surface variant of protein microarrays for autoantibody detection in colon cancer. We identified three novel TAAs: EDIL3, GTF2B and HCK. Combining these three antigens with previously identified TAAs^{2,3,23}, NY-ESO-1²⁴, and p53^{1,9,25}, we studied the humoral response in mouse models developing dysplasia or adenocarcinoma in distal colon. The mouse humoral response gave a reactivity profile similar to that observed in human CRC patients. Moreover, autoantibody titers preceded clinical symptoms and correlated with the type and grade of lesions in all three experimental groups tested, and their levels went parallel to tumor development. The use of AOM- and DSS-only treated mice confirmed the predictive value of the autoantibodies.

Results

A colitis-associated cancer mouse model develops autoantibodies to tumor-associated antigens. We tested the CAC mouse model for the presence of diagnostic autoantibodies. FVB/N mouse strain was selected due to its good susceptibility for tumor formation. After AOM/DSS treatment (Fig. 1a), all mice developed well-differentiated adenocarcinomas in the distal colon, similar to those observed in CRC patients. AOM/DSS-treated mice autoantibody responses were analyzed with p53, STK4/MST1, MAPKAPK3, SRC, and NY-ESO-1 as colon cancer TAAs and two negative controls (GST and Annexin IV) (Fig. 1b). In addition, we also tested EDIL3, GTF2B and HCK, which were here identified after analysis of the immune response of CRC patients and controls with high-density protein microarrays (see Supporting Note 1 for further details, Supplementary Fig. S1, Supplementary Table S1 and Supplementary Table S2).

We used human antigens for the ELISA because of the high amino acid identity with their murine orthologs, going from 76% (p53) to 99% (GTF2B) (Supplementary Table S3). All mouse developed autoantibodies against human TAAs. Best differential values were obtained for p53, GTF2B and STK4/MST1 (mean ELISA values 0.34 versus 0.05, 0.42 versus 0.01, and 0.41 versus 0.01 for AOM/DSS treated mice and non-treated control mice, respectively; with p values <0.001 (Supplementary Fig. S3). Regarding NY-ESO-1, we observed a weak response due, probably, to the lower amino acid identity (29%) with its potential mouse counterpart (Supplementary Table S3). No specific reactivity was observed against control antigens GST and Annexin IV. Therefore, mice also reproduced the lack of response to Annexin IV observed in human CRC patients². Collectively, these results showed that AOM/DSS-treated mice developed a humoral response that followed a specificity pattern similar to human CRC patients.

Autoantibody production is associated to antigen overexpression.

Then, we studied the association between autoantibody induction and changes in protein and gene expression. Distal colon mucosa from AOM/DSS- and vehicle-treated control mice were analyzed for alterations in the expression of TAAs at protein (Fig. 1c) and mRNA level (Fig. 1d). At protein level, a clear overexpression was observed for p53, MAPKAPK3, and EDIL3 in AOM/DSS-treated mice in cancer tissues, whereas MST1/STK4 and GTF2B showed almost no alterations in their expression, and SRC decreased in cancer tissue. Regarding mRNA expression, we observed overexpression for p53, MAPKAPK3 and EDIL3. Again, GTF2B and MST1/STK4 showed almost no alterations in their expression levels. These findings support that autoantibody induction mostly associated to an increase in the expression of TAAs. However, since autoantibodies to SRC, MST1/STK4 and GTF2B were detected without protein or mRNA overexpression, we cannot exclude other reasons (mutations, wrong conformation or altered post-translational modifications ...).

Autoantibody production occurs early in tumor development and before neoplastic lesions. To test the value of autoantibodies for early cancer detection we analyzed the kinetics of antibody synthesis in the AOM/DSS murine model (Fig. 2a). Samples at day 21 post-inoculation of AOM (after the first cycle of DSS), day 42 (after the second cycle) and day 63 (after the third cycle) were analyzed to quantify the antibody response in AOM/DSS-treated ($n = 9$) and control mice ($n = 9$). Autoantibodies were already detected at day 21 and their levels increased in parallel to the progression of the disease from day 21 to day 63 (Fig. 2a). At day 21, an early antibody response against p53 and GTF2B was observed, showing a clear difference between AOM/DSS-treated (mean ELISA value: 0.24 and 0.22, respectively) and non-treated mice (mean: 0.02 and 0.09, respectively), with p value: 0.018 and 0.029, respectively (Fig. 2b and Supplementary Fig. S4). Responses to STK4/MST1 and EDIL3 were lower, suggesting a slower antibody induction for these two TAAs. Thus, antibodies to p53 and GTF2B distinguished cancer from control mice as soon as 21 days after AOM injection and 1 cycle of DSS (Fig. 2b and Supplementary Fig. S4).

Then, we correlated the appearance of dysplasia or neoplastic lesions in the distal colon of AOM/DSS-treated mice with autoantibody detection. At day 21, when autoantibodies were initially detected, there were no noticeable neoplastic lesions or dysplasia in the colon (Fig. 2c). Microadenomas with focal dysplasia in 2 out of 4 animals were firstly detected at day 27, before the second DSS cycle. After the second DSS cycle (day 35), the distal colon of 2 AOM/DSS-treated mice presented clearly infiltrating tumors, arising in more extensive adenomatous areas with high grade dysplasia, which progressed to adenocarcinoma at day 48. At day 63, the adenocarcinoma invaded the muscular layer (Fig. 2c). The presence of adenocarcinomas was coincident with high antibody titers. Collectively, these results indicated that the autoantibody production against TAAs took place before histopathological manifestations and clinical signs were visible and increased in parallel to the progression of the disease. In summary, the humoral response preceded clinical symptoms confirming their capacity for very early CRC diagnosis.

Predictive value in other sporadic cancer models. Since tumor formation occurred in all mice treated with AOM/DSS, we investigated the capacity of autoantibodies for predicting sporadic cancer in animals that do and do not develop cancer. We used two protocols (Fig. 3a): i) 3 cycles of DSS-only administration, without AOM (DSS mice group), and ii) 6 weekly intraperitoneal injections of AOM-only (AOM group) to study the individual contribution of AOM mutagenesis and DSS inflammation in the development and production of autoantibodies. In these two cases not all the animals develop dysplastic symptoms, which facilitates the establishment of correlations between autoantibody production and cancer development.

Mice were histologically examined at days 63 and 250, corresponding to the expected dates for tumor development in DSS and AOM groups, respectively. At day 63, DSS-treated mice showed a whitened, thicker and notably shorter distal intestine, indicating a large bowel inflammation (Fig. 3b). However, histological analysis showed that 3 out of 5 DSS-only mice (DSS 1, DSS 2 and DSS 3) developed intramucosal adenomas in the distal colon, with mild dysplastic lesions or moderate-severe dysplasia (Fig. 3c). On the other hand, DSS 4 showed low grade dysplastic, nonmalignant lesions and DSS 5 showed a normal mucosa. Regarding the AOM-treated group ($n = 7$), two mice inspected at day 63 did not show macro- (Fig. 3b) or microscopic lesions in the distal colon (Fig. 3c). However, at day 250, three mice (AOM2, AOM 3 and AOM 5) showed macroscopical encapsulated and deeply irrigated polypoid cauliflower-like adenomas in the distal colon (Fig. 3d). These three AOM-treated mice presented infiltrating, but non-invasive tumors, where muscularis propria was perforated in AOM 5 mouse (Fig. 3d). All lesions presented cribriform pattern indicating gland degeneration and

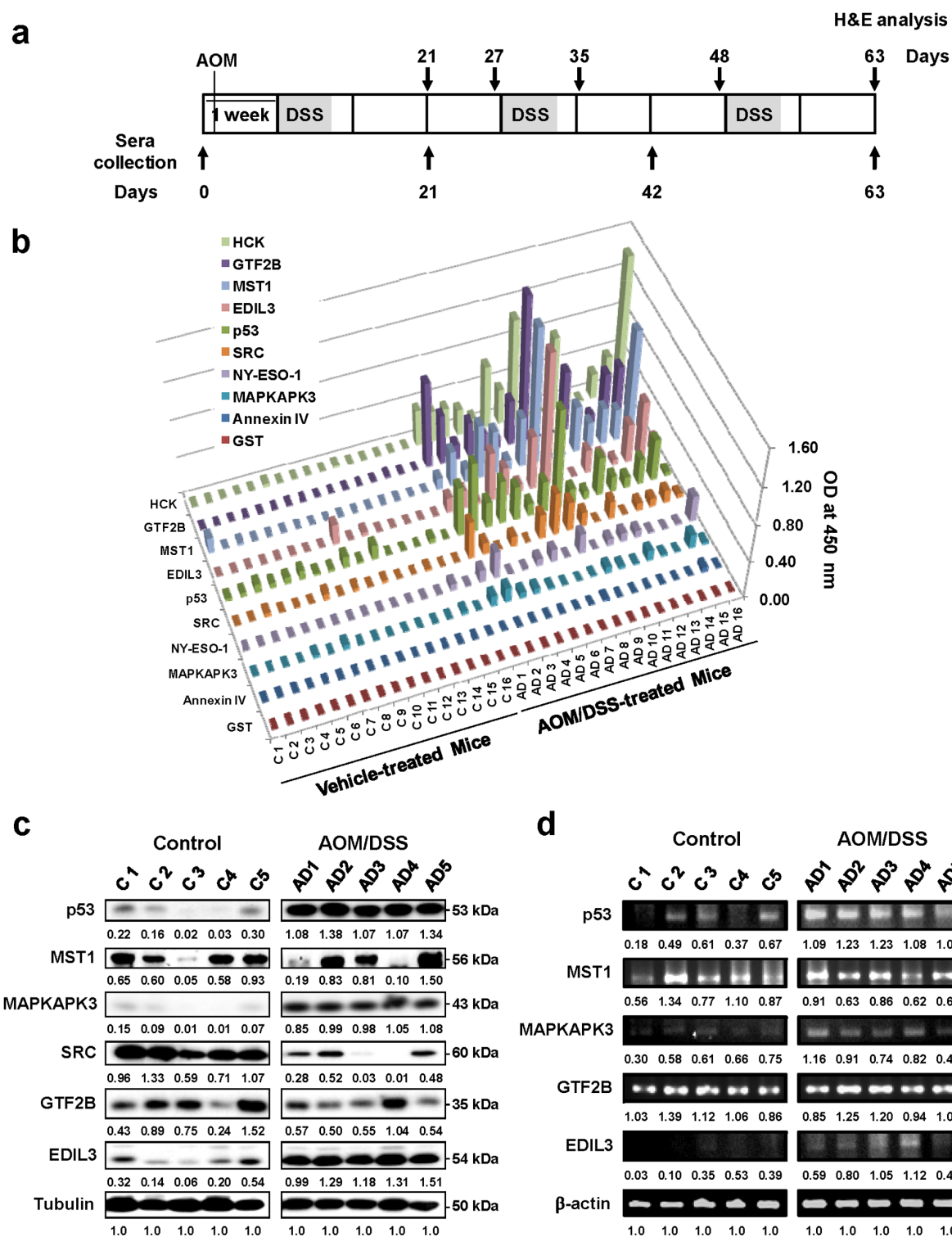


Figure 1 | Presence of autoantibodies in mice with colitis-associated cancer. (a) Schematic overview of the AOM/DSS colorectal cancer model. Each rectangle represents one week. After an initial AOM injection (10 mg/kg), DSS was given in drinking water for a 2.5% final concentration (gray areas) followed by regular water. Histological staining for distal colon morphology and blood collection was performed at indicated days (black arrows). (b) Sera collected after the third DSS cycle (day 63) from 16 AOM/DSS-treated mice developing colorectal adenocarcinoma showed specific reactivity against p53, HCK, GTF2B, EDIL3, MST1/STK4, SRC and MAPKAPK3 with Annexin IV and GST as negative controls. Sera were tested by indirect ELISA using purified human recombinant proteins. NY-ESO-1 showed a weak response. Results are representative of two independent assays. (c) Western blot analysis showed alterations in expression of p53, MAPKAPK3, MST1/STK4, EDIL3, GTF2B and SRC in distal colon from 5 AOM/DSS-treated and 5 control mice. Tubulin was used as loading control in the same gels. (d) Semi-quantitative PCR analysis showing mRNA expression in the distal colon tissue of AOM/DSS- and control mice. β-actin was used as a control. (c, d) WB and semi-quantitative PCR analyses were quantified by densitometry and normalized according to the expression of tubulin and β-actin, respectively. For the cropped images, samples from treated and control animals were run in the same gels under same experimental conditions and processed in parallel. Experiments were run in duplicate.

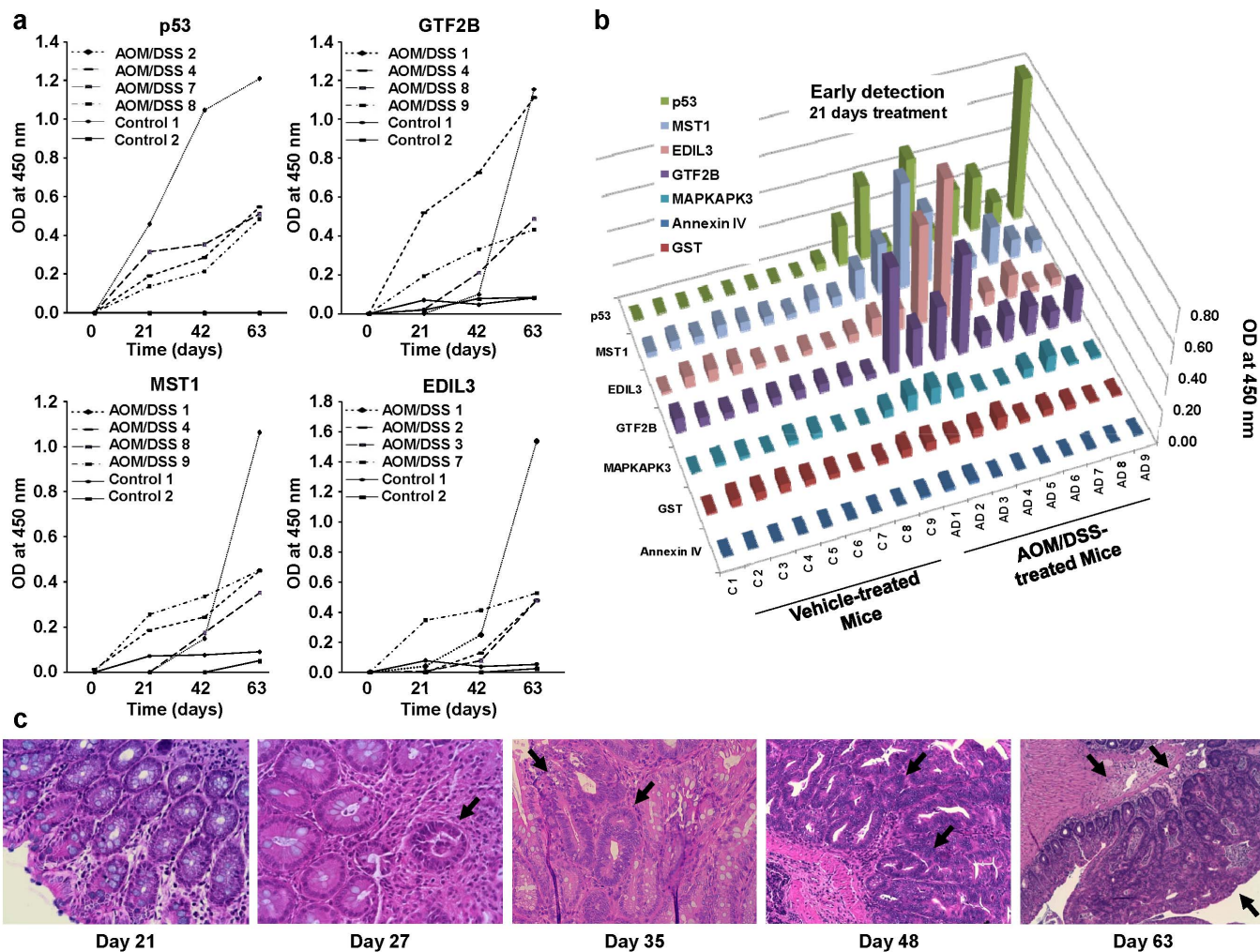


Figure 2 | Antibody response to colorectal cancer TAA is detected before adenoma formation and increases according to tumor progression.

(a) Kinetics of antibody response to p53, GTF2B, MST1/STK4 and EDIL3. Murine sera were tested by indirect ELISA at a 1 : 100 dilution. Autoantibodies showed an increase in autoantibody production parallel to tumor progression. (b) Results representative of two independent assays using murine sera collected at day 21 from 9 AOM/DSS-treated mice and 9 control mice. Annexin IV and GST were used as negative controls. (c) Histological staining of distal colon morphology of AOM/DSS-treated mice at different days to monitor tumor progression. Mice before the second DSS cycle (day 27) showed low levels of dysplasia and early adenoma development (black arrow), with focus of microinfiltration and different degrees of inflammation. During the second cycle of DSS (day 35 to 48), dysplasia became of higher grade in clear-cut adenomatous lesions (black arrow) that progress to well-differentiated adenocarcinoma (black arrow) with invasion of the muscular layer after the third DSS cycle (day 63). Images are shown at 200x magnification.

mitotically active cells (Fig. 3d). Visually, the remaining mice showed small (AOM 1) or no macroscopical lesions (AOM 4). However, by histological staining, AOM 1 and AOM 4 showed small adenomas (Fig. 3d).

Regarding autoantibody production, all mice were tested at day 63 (Fig. 4a) and AOM-treated mice were also tested at day 250 (Fig. 4b). In DSS group, autoantibody levels correlated with the presence of adenomas and dysplasia in the distal colon (Fig. 3b, c). These DSS-treated mouse developed autoantibodies, although at lower titers than AOM/DSS-treated mice (Fig. 4a and Supplementary Fig. S5). At day 63, AOM group did not develop autoantibodies, correlating with the absence of neoplastic lesions in the animals. However, at day 250, a significant presence of autoantibodies was found in those AOM-treated mice presenting colon adenocarcinomas, except AOM 4 mouse presenting a flat adenoma by histological staining and no visually noticeable lesions (Fig. 4b and Supplementary Fig. S6). These results demonstrated the high correlation between colon cancer lesions and autoantibody induction, independently from the tumorigenesis, and confirmed the strong predictive value of the autoantibody response for cancer detection.

Discussion

In this report, we demonstrate that mice treated with different inducible models of colon carcinogenesis developed a humoral immune response, which was similar to that observed in human colon cancer patients. Moreover, the induction of autoantibodies in AOM/DSS-treated mice occurred at very early stages and was parallel to the progression of the disease. Autoantibodies were detected before the onset of cancer lesions and the reactivity pattern was analogous to the humoral immune response found in human colorectal cancer patients. Experiments with DSS-only and AOM-only mice, where not all animals developed tumors, confirmed the high correlation between tumor formation and autoantibody induction. Only those mice showing adenomas and malignant dysplastic lesions developed significant levels of autoantibodies. In this regard, some mice that developed bowel inflammation without neoplasia, particularly in the DSS-only model, failed to develop antibodies. Besides, the level of autoantibodies in these two variants was lower than in AOM/DSS-treated mice and suggests that different treatments might result in variable responses, probably due to subtle differences in the TAA being present in the swollen, dysplastic tissue, adenoma or colorectal cancer tumors.

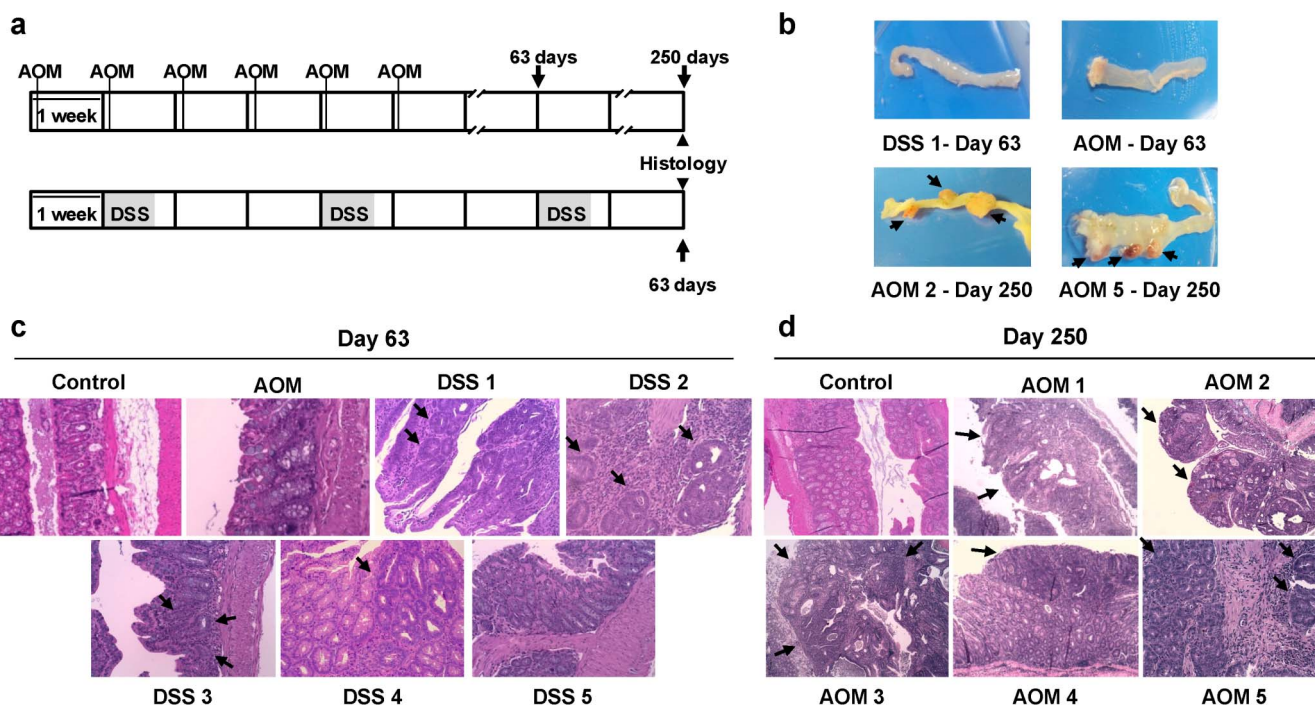


Figure 3 | DSS-only and AOM-only models of sporadic colon carcinogenesis. (a) Top, AOM (10 mg/kg) was weekly injected during six weeks. Bottom, fresh 2.5% DSS was given in drinking water during five-day cycles (gray areas) followed by regular drinking water for 16 days. Blood samples were collected at the end of the protocols and also for AOM-treated mice at day 63. (b) Representative images of distal colon macroscopic appearance of DSS-treated (day 63) and AOM-treated mice at day 63 and 250. Tumors are highlighted with black arrows. (c) Representative haematoxylin/eosin staining sections of distal colon morphology of DSS- and AOM-treated mice and control mice. No significant changes were observed for AOM-treated mouse at day 63. DSS-treated mice showed presence of adenomas and different grade of dysplasia (DSS 1, DSS 2 and DSS 3) at day 63, whereas DSS 4 animal showed low grade nonmalignant dysplastic lesions and DSS 5 showed no changes respect to normal mucosa. (d) At day 250, three AOM-treated mice showed infiltrating but non-invasive tumors (AOM 2, AOM 3 and AOM 5), whereas the remaining animals (AOM 1 and AOM 4) showed small flat non-polypoid adenomas with dysplasia. (c, d) Black arrows highlight the observed lesions. Images are shown at 200x magnification.

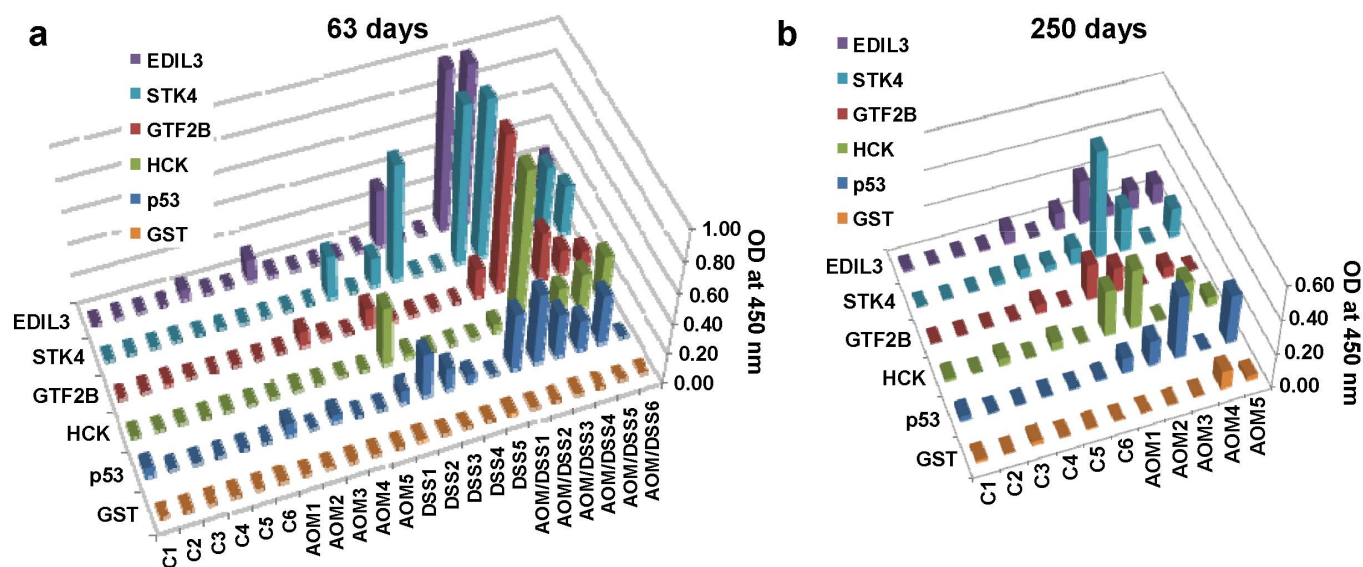


Figure 4 | Presence of autoantibodies in AOM- or DSS-only treated FVB/N mice correlate with the presence of cancer-like lesions. Sera collected from DSS-, AOM- and vehicle-treated control mice were investigated for autoantibodies to p53, MST1/STK4, EDIL3, GTF2B and HCK by indirect ELISA and GST as negative control. Results are representative of two independent assays. (a) ELISA values at day 63 indicated the presence of significant levels of autoantibodies in animals of the DSS-treated mice group that showed adenomas with mild or moderate-severe dysplasia in the distal colon. DSS 4 and DSS 5 animals, showing non-malignant lesions and normal mucosa, respectively, as well as control group and AOM-treated mice did not develop autoantibodies at day 63. (b) ELISA values at day 250 indicated the presence of significant levels of autoantibodies in AOM-treated mice in comparison to control mice.



The utility of autoantibodies for early detection of cancer has been questioned for a long time, as the access to preclinical collection of sera is difficult. In general, sample collection from the same patient, before and after tumor development and during all tumor stages, is not generally available, making almost impossible to determine the exact moment when the autoantibodies appear and their correlation with tumor progression. Only a few reports described the use of autoantibodies in early diagnosis of cancer^{10,26}. Autoantibodies to annexin I, 14-3-3 Theta and LAMR1 were detected in pre-diagnostic lung cancer sera using sera collected 1 year before the diagnosis of lung cancer²⁶. Furthermore, antibodies to p53, c-myc and MUC1 were detected in women between 7 and 27 months before breast cancer was diagnosed¹⁰. However, no direct link between antibody generation and early dysplastic events was previously reported. Here, by using the AOM/DSS murine model, we provide evidence of the immediateness of the antibody response, detectable at day 21 after neoplastic transformation. This very early response confirms the exquisite sensitivity of the immune system and suggests that only a few tumor cells, undetectable by other means, are required for local antigen processing by the immune system.

Genetic homogeneity and the lack of environmental mutagens in the AOM/DSS mouse model avoid the high variability observed in the human antibody response and facilitate the production of reproducible results from mouse to mouse. Our study also supports that murine sera could be used for testing different TAAs coming from different studies, enabling the standardization and validation of TAA selection. An exception to this could be the cancer-testis TAAs. Due to the absence or low homology of murine orthologs; in fact, we noticed a low response to NY-ESO-1.

The role of autoantibodies in cancer is still unclear. It is unknown if they play a cancer-promoting role, an anti-tumoral effect, or they are an epiphenomenon associated to inflammation and tumor progression²⁷. The capacity of the mouse model to mimic extremely well the human humoral response to TAAs paves the way to dissect the molecular mechanisms of the autoantibody response in cancer patients. Interestingly, one characteristic of the AOM/DSS model is the very low frequency of mutations in p53^{13,28–30}. However, we and others have observed significant increases in p53 expression^{29–31}, which might be explained by accumulation of mutant p53 due to lower degradation (Fig. 1b). Previous observations showed that there were not significant differences between mutant forms or wild-type p53 for autoantibody recognition in human sera³². Additional factors such as incorrect folding, incorrect conformation or post-translational modifications may account for this reactivity.

Inflammation is a common event in tumor development, especially in the gastrointestinal tract³³. Little is known about the link between inflammation, autoimmunity and autoantibody production in cancer. Murine colon cancer models might help to understand the molecular basis of this process and study the association between inflammation, autoantibody production and cancer progression. The AOM/DSS models are characterized by the activation of NF- κ B, STAT3 and expression of high levels of IL-6³⁴. Activation of IL-6 receptor results in different signaling events that lead to the induction of autoimmunity mediated by Th17 cells³⁵. Therefore, IL-6 might promote these autoantibody responses in cancer. The characterization of these events in cancer autoimmunity will require further studies. According to our results, inflammation seems to be a driver of autoantibody induction, although not sufficient in some cases.

As main conclusion of this study, we have demonstrated the very early induction of autoantibodies in cancer, which confirms the diagnostic value of this approach for pre-clinical detection of human colon cancer. The presence of autoantibodies was associated to the neoplastic changes, independently from their origin. Thus, autoantibody tests could be recommended to identify cancer-carrier individuals in a first screening of the population. These findings should be further confirmed by colonoscopy and/or other imaging techniques.

Methods

Clinical Information of serum samples for protein microarrays and statistical analysis. The Institutional Ethical Review Boards of the Centro de Investigaciones Biológicas (CIB) and the Spanish National Research Council (CSIC) approved this study on biomarker discovery in colorectal cancer. See supplementary online data for additional information.

Murine colon cancer models. For the AOM/DSS model, we followed a published protocol³⁶, with minor modifications. Briefly, FVB/N mice (4–6 weeks-old) were weighed and given a single intraperitoneal injection of azoxymethane (AOM; 10 mg/kg) or vehicle (PBS). Five days later, animals received either 2.5% DSS or normal drinking water, respectively. Chronic colitis and colon cancer were induced after three cycles of DSS treatment, which consisted of 5 days of 2.5% fresh DSS followed by 16 days of normal drinking water. Blood was collected at the starting day of the experiment and 1 week after every DSS cycle.

To test separately the effects of AOM and DSS in the production of autoantibodies and the development of cancer-like lesions in the FVB/N strain we followed two protocols: i) one intraperitoneal injection of AOM (10 mg/kg) once a week for 6 weeks and then maintained up to 250 days, and ii) 3 cycles of 2.5% DSS as above without the AOM injection and maintained during the same time than AOM/DSS murine model (63 days). Blood was collected at the starting day and at the endpoint of the experiments, or alternatively, at indicated times. We euthanized several treated and control animals at the indicated times to monitor tumor progression by histological staining. In those specific days, their blood and tissues were harvested. At the end of the protocols, we collected samples for all mice. Distal colons from all mice were longitudinally cut, rinsed twice with ice-cold PBS, cut in small pieces and either frozen at -80°C for RNA and protein extraction or fixed in 10% buffered formalin overnight to perform histological staining after paraffin embedding. Serum samples were processed according to standard procedures.

Protein expression and RNA extraction. cDNA encoding for full-length human genes EDIL3, GTF2B and HCK in pDONR221 were obtained from the Plasmid repository (Harvard Institute of Proteomics) and, then, subcloned into pET28a (Novagen) for protein expression. TAAs were expressed in bacteria and purified according to previous studies²³. p53 and NY-ESO-1 expressed as GST fusions in baculovirus were purchased from Interchim and Thermo Scientific, respectively.

RNA was extracted from colon distal tissue from AOM/DSS- and vehicle-treated control mice with the AllPrep DNA/RNA Mini Kit (Qiagen).

ELISA experiments. ELISA was carried out as previously described²³. Briefly, microtiter plates (Maxisorp, Nunc) were coated overnight with 0.3 μg of the purified recombinant proteins, using GST and human Annexin IV as negative controls in 50 μl of PBS. After washing three times with PBS, plates were blocked with 3% skimmed milk in PBS (MPBS) for 2 h at room temperature. Then, mouse serum samples (dilution, 1:100 in 3% MPBS) were incubated for 2 h at room temperature. After washing, peroxidase-labeled anti-mouse IgG (Jackson laboratories) (dilution, 1:500 in 3% MPBS) was added for 2 h at room temperature. Then, the signal was developed with 3, 3', 5, 5'-tetramethylbenzidine substrate for 10 min (Sigma). The reaction was stopped with 1 M HCl, and absorption measured at 450 nm.

All *p* values were derived from a one-tailed statistical test assuming unequal variances to assess whether the means of groups were statistically different from each other. *p* values <0.05 were considered statistically significant. Each individual marker and the combination of biomarkers were evaluated from murine ELISA data sets by ROC curve analysis. The corresponding AUC, sensitivity and specificity were calculated using JMP® 10 (SAS).

Western blot analysis. Protein extracts from colorectal cancer cells were prepared and quantified with the 2D-Quant kit (GE Healthcare) according to previously published protocols^{23,37}. Then, 25 μg of each protein extract were run in parallel using 10% SDS-PAGE. For immunoblotting, proteins were transferred to nitrocellulose membranes (Hybond-C extra) using wet transfer equipment (Bio-Rad). After blocking, membranes were incubated with specific mono- or polyclonal antibodies against the selected proteins. Membranes were incubated at optimized dilutions with primary antibodies followed by incubation with either HRP-anti-mouse IgG (Pierce) at 1:5000 dilution or HRP-anti-rabbit IgG (Sigma) at 1:5000 dilution. Specific reactive proteins were visualized with SuperSignal West Pico Maximum Sensitivity Substrate (Pierce).

The abundance of the proteins in western blot assays was quantified by densitometry using Quantity One 1D Analysis Software v4.6 (Bio-Rad Laboratories).

Semi-quantitative RT-PCR analysis. PCRs were performed as previously described^{38,39}. Briefly, 1 μg of RNA from distal colon tissue from AOM/DSS-treated and vehicle-treated control mice were reverse transcribed by using Superscript III (Invitrogen). Oligonucleotides for murine TAAs were designed by using PrimerBlast (Supplementary Table S4). For RT-PCR analysis, 0.8 μl of cDNA was subjected to PCR using KOD DNA polymerase (Novagen) in a total volume of 20 μl to amplify murine p53, GTF2B, EDIL3, STK4/MST1 and MAPKAPK3 with specific primers (Supplementary Table S4). The PCR consisted of 30 cycles of amplification at 68°C of annealing temperature. Finally, 5 μl of the previous reaction were loaded onto a 1.5% agarose gel. Murine β -actin was used as control. Semi-quantitative PCR analyses were quantified by densitometry using Quantity One 1D Analysis Software v4.6 (Bio-Rad Laboratories).



Immunohistochemistry. Distal colon from AOM-, DSS-, AOM/DSS- and vehicle-treated control mice were fixed in buffered formaldehyde and paraffin-embedded. Immunohistochemistry was performed on 6 μ m sections of the blocks following an automated method (Dako Autostainer). We counterstained the slides with hematoxylin. In all cases, an external negative control was included.

- Scanlan, M. J. *et al.* Characterization of human colon cancer antigens recognized by autologous antibodies. *Int J Cancer* **76**, 652–658 (1998).
- Babel, I. *et al.* Identification of tumor-associated autoantigens for the diagnosis of colorectal cancer in serum using high density protein microarrays. *Mol Cell Proteomics* **8**, 2382–2395 (2009).
- Babel, I. *et al.* Identification of MST1/STK4 and SULF1 proteins as autoantibody targets for the diagnosis of colorectal cancer by using phage microarrays. *Mol Cell Proteomics* **10**, M110 001784 (2011).
- Wang, X. *et al.* Autoantibody signatures in prostate cancer. *N Engl J Med* **353**, 1224–1235 (2005).
- Chatterjee, M. *et al.* Diagnostic markers of ovarian cancer by high-throughput antigen cloning and detection on arrays. *Cancer Res* **66**, 1181–1190 (2006).
- Hudson, M. E., Pozdnyakova, I., Haines, K., Mor, G. & Snyder, M. Identification of differentially expressed proteins in ovarian cancer using high-density protein microarrays. *Proc Natl Acad Sci U S A* **104**, 17494–17499 (2007).
- Chen, G. *et al.* Autoantibody profiles reveal ubiquitin 1 as a humoral immune response target in lung adenocarcinoma. *Cancer Res* **67**, 3461–3467 (2007).
- Chapman, C. J. *et al.* Autoantibodies in lung cancer: possibilities for early detection and subsequent cure. *Thorax* **63**, 228–233 (2008).
- Crawford, L. V., Pim, D. C. & Bulbrook, R. D. Detection of antibodies against the cellular protein p53 in sera from patients with breast cancer. *Int J Cancer* **30**, 403–408 (1982).
- Chapman, C. *et al.* Autoantibodies in breast cancer: their use as an aid to early diagnosis. *Ann Oncol* **18**, 868–873 (2007).
- Casal, J. I. & Barderas, R. Identification of cancer autoantigens in serum: toward diagnostic/prognostic testing? *Mol Diagn Ther* **14**, 149–154 (2010).
- Neufert, C., Becker, C. & Neurath, M. F. An inducible mouse model of colon carcinogenesis for the analysis of sporadic and inflammation-driven tumor progression. *Nat Protoc* **2**, 1998–2004 (2007).
- De Robertis, M. *et al.* The AOM/DSS murine model for the study of colon carcinogenesis: From pathways to diagnosis and therapy studies. *J Carcinog* **10**, 9 (2011).
- Okayasu, I. *et al.* Dysplasia and carcinoma development in a repeated dextran sulfate sodium-induced colitis model. *J Gastroenterol Hepatol* **17**, 1078–1083 (2002).
- Corpet, D. E. & Pierre, F. How good are rodent models of carcinogenesis in predicting efficacy in humans? A systematic review and meta-analysis of colon chemoprevention in rats, mice and men. *Eur J Cancer* **41**, 1911–1922 (2005).
- Okayasu, I. *et al.* A novel method in the induction of reliable experimental acute and chronic ulcerative colitis in mice. *Gastroenterology* **98**, 694–702 (1990).
- Clapper, M. L., Cooper, H. S. & Chang, W. C. Dextran sulfate sodium-induced colitis-associated neoplasia: a promising model for the development of chemopreventive interventions. *Acta Pharmacol Sin* **28**, 1450–1459 (2007).
- Cooper, H. S., Murthy, S., Kido, K., Yoshitake, H. & Flanagan, A. Dysplasia and cancer in the dextran sulfate sodium mouse colitis model. Relevance to colitis-associated neoplasia in the human: a study of histopathology, B-catenin and p53 expression and the role of inflammation. *Carcinogenesis* **21**, 757–768 (2000).
- Nambiar, P. R. *et al.* Preliminary analysis of azoxymethane induced colon tumors in inbred mice commonly used as transgenic/knockout progenitors. *Int J Oncol* **22**, 145–150 (2003).
- Greten, F. R. *et al.* IKK β links inflammation and tumorigenesis in a mouse model of colitis-associated cancer. *Cell* **118**, 285–296 (2004).
- Suzuki, R., Kohno, H., Sugie, S. & Tanaka, T. Sequential observations on the occurrence of preneoplastic and neoplastic lesions in mouse colon treated with azoxymethane and dextran sodium sulfate. *Cancer Sci* **95**, 721–727 (2004).
- Terzic, J., Grivennikov, S., Karin, E. & Karin, M. Inflammation and colon cancer. *Gastroenterology* **138**, 2101–2114 e2105 (2010).
- Barderas, R. *et al.* An optimized predictor panel for colorectal cancer diagnosis based on the combination of tumor-associated antigens obtained from protein and phage microarrays. *J Proteomics* **75**, 4647–4655 (2012).
- Scanlan, M. J. *et al.* Cancer-related serological recognition of human colon cancer: identification of potential diagnostic and immunotherapeutic targets. *Cancer Res* **62**, 4041–4047 (2002).
- Soussi, T. p53 Antibodies in the sera of patients with various types of cancer: a review. *Cancer Res* **60**, 1777–1788 (2000).
- Qiu, J. *et al.* Occurrence of autoantibodies to annexin I, 14-3-3 theta and LAMR1 in prediagnostic lung cancer sera. *J Clin Oncol* **26**, 5060–5066 (2008).
- Kobold, S., Lutkens, T., Cao, Y., Bokemeyer, C. & Atanackovic, D. Autoantibodies against tumor-related antigens: incidence and biologic significance. *Hum Immunol* **71**, 643–651 (2010).
- Takahashi, M. & Wakabayashi, K. Gene mutations and altered gene expression in azoxymethane-induced colon carcinogenesis in rodents. *Cancer Sci* **95**, 475–480 (2004).
- Nambiar, P. R. *et al.* Genetic signatures of high- and low-risk aberrant crypt foci in a mouse model of sporadic colon cancer. *Cancer Res* **64**, 6394–6401 (2004).
- Rosenberg, D. W., Giardina, C. & Tanaka, T. Mouse models for the study of colon carcinogenesis. *Carcinogenesis* **30**, 183–196 (2009).
- Cui, X. *et al.* Resveratrol suppresses colitis and colon cancer associated with colitis. *Cancer Prev Res (Phila)* **3**, 549–559 (2010).
- Anderson, K. S. *et al.* Application of protein microarrays for multiplexed detection of antibodies to tumor antigens in breast cancer. *J Proteome Res* **7**, 1490–1499 (2008).
- Hanahan, D. & Weinberg, R. A. Hallmarks of cancer: the next generation. *Cell* **144**, 646–674 (2011).
- Grivennikov, S. *et al.* IL-6 and Stat3 are required for survival of intestinal epithelial cells and development of colitis-associated cancer. *Cancer Cell* **15**, 103–113 (2009).
- Neurath, M. F. & Finotto, S. IL-6 signaling in autoimmunity, chronic inflammation and inflammation-associated cancer. *Cytokine Growth Factor Rev* **22**, 83–89 (2011).
- Wirtz, S., Neufert, C., Weigmann, B. & Neurath, M. F. Chemically induced mouse models of intestinal inflammation. *Nat Protoc* **2**, 541–546 (2007).
- Pelaez-Garcia, A. *et al.* FGFR4 role in epithelial-mesenchymal transition and its therapeutic value in colorectal cancer. *PLoS One* **8**, e63695 (2013).
- Barderas, R., Bartolome, R. A., Fernandez-Acenero, M. J., Torres, S. & Casal, J. I. High expression of IL-13 receptor alpha2 in colorectal cancer is associated with invasion, liver metastasis, and poor prognosis. *Cancer Res* **72**, 2780–2790 (2012).
- Bartolome, R. A. *et al.* Cadherin-17 interacts with alpha2beta1 integrin to regulate cell proliferation and adhesion in colorectal cancer cells causing liver metastasis. *Oncogene* (2013).

Acknowledgements

R. Barderas was a JAE-DOC fellow of the CSIC and is currently a recipient of the Ramón y Cajal programme of the MINECO. R. Villar-Vázquez was a recipient of a FPU fellowship of the Ministry of Education of Spain. Alberto Peláez was a recipient of a FPI fellowship from the MINECO. Sofia Torres was a fellow from the Juan de la Cierva programme (MINECO). This study was supported by grant BIO2012-31023 from the MINECO, a grant to established research groups of the Asociación Española Contra el Cancer and the grant S2010/BMD-2344/Colomics2 from Comunidad de Madrid.

Author contributions

J.I.C. and R.B. designed the study; R.B., R.V.V., M.J.F.A., I.B., S.T. and A.P.G. did the experiments. All authors did data analysis and interpretation. J.I.C. and R.B. wrote the manuscript.

Additional information

Supplementary information accompanies this paper at <http://www.nature.com/scientificreports>

Competing financial interests: The authors declare no competing financial interests.

How to cite this article: Barderas, R. *et al.* Sporadic colon cancer murine models demonstrate the value of autoantibody detection for preclinical cancer diagnosis. *Sci. Rep.* **3**, 2938; DOI:10.1038/srep02938 (2013).



This work is licensed under a Creative Commons Attribution-NonCommercial-NoDerivs 3.0 Unported license. To view a copy of this license, visit <http://creativecommons.org/licenses/by-nc-nd/3.0>